DALTON
FULL PAPER

A new type of zinc sulfide cluster: $[Zn_{10}S_7(py)_9(SO_4)_3]\cdot 3H_2O$

Basem Ali, Ian G. Dance,*,† Don C. Craig and Marcia L. Scudder

School of Chemistry, University of New South Wales, Sydney 2052, Australia

The cluster $[Zn_{10}S_7(py)_9(SO_4)_3]\cdot 3H_2O$ has been synthesized by reaction of the product of thermolysis of $[NMe_4]_4[Zn_{10}S_4(SPh)_{16}]$ [believed to be $Zn_{10}S_4(SPh)_{12}$] with pyridine containing Na_2SO_4. The compound was characterised by X-ray crystallography: monoclinic space group $P2_1/c$, $a = 11.279(6)$, $b = 23.419(6)$, $c = 27.26(1)$ Å, $\beta = 107.74(2)$, $Z = 4$. This cluster is unprecedented in its architecture, and for its combination of sulfide, sulfate and pyridine ligands. It has pseudo-three-fold symmetry. In the core the ten Zn atoms are arrayed as a central Zn_4 tetrahedron on the three-fold axis, crowned with a slightly puckered Zn_6 hexagon around the axial Zn atom of the Zn_4 tetrahedron. The Zn_4 tetrahedron contains μ_4-S^{2-}. The axial Zn atom of the Zn_4 tetrahedron is connected to the Zn_6 hexagon through three μ_3-S^{2-} ligands. Another three μ_3-S^{2-} ligands connect the base of the Zn_4 tetrahedron to the Zn_6 hexagon. Each SO_4^{2-} ion bridges three Zn atoms: two from an edge of the hexagon and one basal Zn atom of the tetrahedron. All Zn atoms have distorted tetrahedral co-ordination, completed by terminal pyridine ligands on all except the axial Zn atom. The crystal supramolecularity is a stacking of the clusters such that three axially directed pyridine ligands (on the basal Zn_4 atoms) nestle amongst six equatorially directed pyridine ligands (on the Zn_6 hexagon) of an adjacent molecule. Water molecules are hydrogen bonded to SO_4^{2-} and μ_3-S atoms. The Zn–S connectivity in this cluster is different from that in the cubic or hexagonal lattices of ZnS, and from that in known $M_8S(SR)_{16}$, $M_{17}S_4(SR)_{28}$ and $M_{10}(SR)_{10}$ clusters formed by Group 12 metals.

In the chemistry of metal sulfide clusters[1] the compositions and structures known for zinc include the clusters $[Zn_{10}S_4(SPh)_{16}]^{4-}$ and $[Zn_{10}S_4(SPh)_{12}X_4]^{4-}$, with X = Cl, Br or I,[2–5] together with derivatives $[Zn_{10}S_4(S_2C_6H_3Me_2\text{-}2,3)_8]^{4-}$[6] and $[Zn_{10}S_4(SEt)_{12}(lut)_4]$[7] (lut = lutidine, 2,6-dimethylpyridine) all of which have fused tetraadamantanoid structures in which the Zn–S array is a fragment of the cubic (sphalerite) lattice of non-molecular ZnS. A smaller cluster with one bridging sulfide ligand is $[Zn_4S(S_2AsMe_2)_6]$.[8] The monoadamantanoid cage compound $[Zn_4(SPh)_{10}]^{2-}$[9–11] (and substituted derivatives[12,13]) can be regarded as organosulfide relatives.[14] We have reported the thiolate cluster with central chloride, $[Zn_8Cl(SPh)_{16}]^-$,[15] and the linked adamantanoid clusters in $[Zn_4(SPh)_8(MeOH)]$.[16] Small zinc thiolate (cysteinyl) clusters are essential components of the metallothionein proteins[17–19] which regulate the levels of class B metals in animals. The reactions and rearrangements of metal chalcogenide clusters such as these are being investigated informatively by electrospray mass spectrometry.[20–22]

While many of the above zinc sulfide cluster systems have cadmium homologues,[1] zinc is different in its formation of organozinc–thiolate clusters by reaction of organozinc compounds with sulfur. Examples of these include $[Zn_5Me_5(SBu^t)_5]$, $[Zn_8Me_8(SPr^i)_8]$[23,24] and $[Zn_{10}Et_{10}(SEt)_{10}]$.[25]

Bulk ZnS is a photoresponsive semiconductor, and these electronic properties are subject to size quantisation which is a dependence of the valence and conduction band energies, and the band gap, on the particle size.[26–31] Therefore there have been many investigations of the preparations and properties of nanoscale ZnS particles, prepared as monodisperse colloids by hydrolysis of thioacetamide to generate sulfide,[32] and as organosols by treatment of zinc acetate in dmf or dmso with H_2S.[33] Nanocrystallites of ZnS have been stabilised in micelles,[34,35] lipid bilayer membranes[36,37] and polymers.[38] Applications as catalysts for photochemical reactions have been reported.[39] The ZnS clusters and surfaces have been investigated theoretically.[40,41]

In all of the above work the ligands or environment which terminate the ZnS cluster are significant in influencing size and structure. In this paper we report a ZnS cluster in which the terminal ligands are pyridine (rare in existing knowledge of ZnS clusters), and with a geometrical structure type not previously observed.

† E-Mail: I.Dance@unsw.edu.au

Experimental

Preparation of $[Zn_{10}S_7(py)_9(SO_4)_3]\cdot 3H_2O$

The reactions were done in an atmosphere of nitrogen using Schlenk techniques. The salt $[NMe_4]_4[Zn_{10}S_4(SPh)_{16}]$ was prepared by the literature method.[2] The precursor for the preparation of $[Zn_{10}S_7(py)_9(SO_4)_3]\cdot 3H_2O$ is a white solid obtained by thermolysis of $[NMe_4]_4[Zn_{10}S_4(SPh)_{16}]$ at 250 °C under dynamic vacuum for 1 h: this is believed to have the composition $Zn_{10}S_4(SPh)_{12}$, by analogy with the cadmium homologue.[42,43]

A solution of anhydrous Na_2SO_4 (1.00 g, 10 mmol) in pyridine (200 cm^3) was prepared. (Presumed) $Z_{10}S_4(SPh)_{12}$ (0.13 g) was treated with this solution (12 cm^3) of Na_2SO_4 in pyridine, at room temperature, yielding a clear solution. Sulfur (0.03 g, 0.2 mmol S_8) was added with stirring. The mixture was stirred and heated to *ca*. 70 °C for about 2 min until all of the sulfur dissolved. The clear yellow solution was cooled to ambient temperature, layered in air with acetone (2 cm^3), and allowed to stand at room temperature. Colourless blocky crystals [0.045 g, 37% based on $Zn_{10}S_4(SPh)_{12}$] grew during 2 d. The composition was determined by single crystal diffraction analysis. The homogeneity of the preparative sample was checked by comparison of its X-ray diffraction pattern with that calculated for the single crystal structure. Powder diffraction pattern (*d*/Å, intensity): 12.66s, 11.19s, 10.80vs, 9.66s, 9.02m, 7.97m, 7.60m, 4.19m, 3.67s, 3.60s, 3.34s, 2.97s and 2.80s.

Crystallography

A single crystal from the preparative mixture was mounted on an Enraf-Nonius CAD-4 diffractometer, and data collected at room temperature. Crystallographic details are provided in Table 1. Absorption corrections were applied using analytical methods.[44] The structure was solved by direct phasing and Fourier methods in the normal way, without complications.

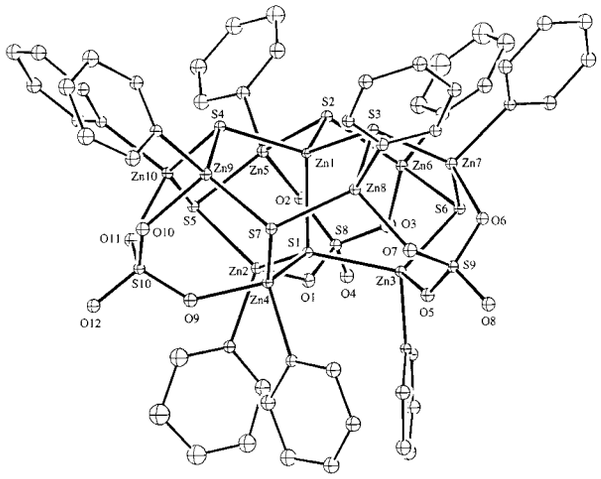

Fig. 1 Crystallographic atom labels for the core atoms of $[Zn_{10}S_7(py)_9(SO_4)_3]$. The pyridine N atoms bonded to Zn*x* are labelled NP($x - 1$), $x = 2$–10 in the supplementary material. Pyridine C atoms are labelled around each ring as C*p*NP*q*, $p = 1$–5, $q = 1$–9

Reflection weights used were $1/\sigma^2(F_o)$ with $\sigma(F_o)$ derived from $\sigma(I_o) = [\sigma^2(I_o) + (0.04I_o)^2]^{\frac{1}{2}}$. The pyridine rings were refined with imposed *mm*2 symmetry,[45] with hydrogen atoms at calculated positions (C–H 1 Å). The final *R* factor was 0.034 for 4610 observed reflections.

CCDC reference number 186/918.

Results

Synthesis

The preparation of $[Zn_{10}S_7(py)_9(SO_4)_3]\cdot 3H_2O$ was initially serendipitous, from a reaction mixture of $Zn_{10}S_4(SPh)_{12}$ and S_8 in pyridine, with no intentionally added sulfate. The composition of the compound which crystallised was revealed by single-crystal structure determination, and the homogeneity of the whole of the crystalline product confirmed by powder X-ray diffraction. In the initial preparation the source of the sulfate was apparently contamination of the solvent pyridine by traces of dissolved metal sulfate used as drying agent. Subsequent experiments using controlled solutions of sodium sulfate in pyridine yielded a reproducible synthesis of $[Zn_{10}S_7(py)_9(SO_4)_3]\cdot 3H_2O$. We also investigated the possibility that the sulfate was generated by oxidation of sulfide, but reactions in the presence of air and without added sulfate did not yield $[Zn_{10}S_7(py)_9(SO_4)_3]\cdot 3H_2O$. The preferred preparative method is anaerobic.

Numerous experiments have been undertaken in attempts to develop a more rational synthesis of $[Zn_{10}S_7(py)_9(SO_4)_3]\cdot 3H_2O$. Most of the strategies involved logical zinc salt precursors, and various sources of sulfide, in solvent systems containing pyridine, and temperature variation. Solutions of $ZnSO_4$ or $ZnSO_4$–$Zn(NO_3)_2$ in the target proportions, in various mixtures of methanol–pyridine, were used. Sources of the sulfide ligand which have been used include NaSH, $Na_2S\cdot 9H_2O$, H_2S gas, and polysulfide compounds in the presence of reducing agents $NaBH_4$ and PhS^-. In another series of reactions, precursors containing thiolate and more akin to $Zn_{10}S_4(SPh)_{12}$ were investigated: these included $Zn(SPh)_2$, $[NMe_4]_2[Zn(SPh)_4]$ and $[NMe_4]_2[Zn_4(SPh)_{10}]$, again using the solvent mixture methanol–pyridine and other aprotic solvents, with different sources of sulfide ligand. The compound $[Zn(py)_2S_6]$,[46–48] in the presence of a reducing agent (*e.g.* PhSH), was used as a logical source of both the zinc ions and sulfide ligand. However none of these preparative mixtures yielded crystalline $[Zn_{10}S_7(py)_9(SO_4)_3]\cdot 3H_2O$.

Since zinc is spectroscopically silent while the NMR of $^{113,111}Cd$ is very informative, we also explored the formation of the cadmium homologue in solution, so far without success.

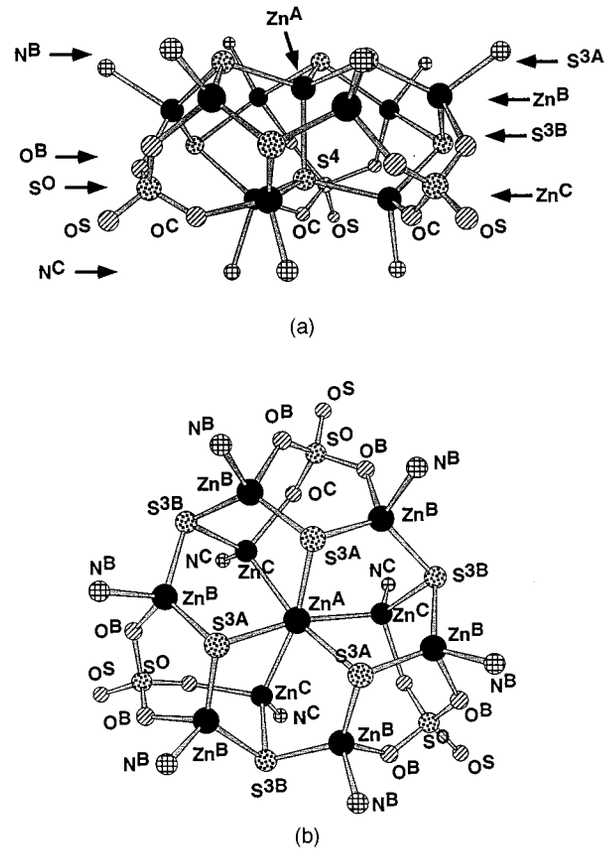

Fig. 2 Atom-type labels for $[Zn_{10}S_7(py)_9(SO_4)_3]$, shown (a) with the same orientation as in Fig. 1, and (b) along the pseudo-three-fold axis. Numbers in the superscripts are co-ordination numbers. Correspondence with the crystallographic atom labels is: Zn^A = Zn1; Zn^B = Zn5, Zn6, Zn7, Zn8, Zn9, Zn10; Zn^C = Zn2, Zn3, Zn4; S^4 = S1; S^{3A} = S2, S3, S4; S^{3B} = S5, S6, S7; S^O = S8, S9, S10; N^B = NP4, NP5, NP6, NP7, NP8, NP9; N^C = NP1, NP2, NP3; O^S = O4, O8, O12; O^B = O2, O3, O6, O7, O10, O11; O^C = O1, O5, O9. In (b) only one of each atom type is labelled, and S^4 is obscured by Zn^A

Cluster structure

The cluster $[Zn_{10}S_7(py)_9(SO_4)_3]$ has a $Zn_{10}S_7$ core, capped by three tridentate SO_4^{2-} ligands and terminated by nine pyridine ligands. The aggregate of the core and the SO_4^{2-} ligands has pseudo-three-fold symmetry, which is maintained in the locations of the pyridine rings but not in their conformations around the Zn–N bonds. One Zn atom lies on the three-fold axis, surrounded by six Zn atoms in a slightly puckered hexagon, while the other three Zn atoms complete an approximate tetrahedron with the axial Zn as apex. All Zn atoms other than the axial Zn have terminal pyridine co-ordination. All sulfide ions are bridging, as three types, and the sulfate ions function as tripodal tridentate ligands around the equatorial belt of the molecule.

Fig. 1, with the crystallographic atom labels, shows the full molecule from the side, with the pseudo-three-fold axis vertical. In order to simplify the description and rationalisation of the molecular structure of the cluster, labels based on the different *types* of atoms under assumed three-fold symmetry are used, and are presented in Fig. 2. The core is built around a $(\mu_4\text{-S})Zn_4$ tetrahedron oriented along the pseudo-three-fold axis, with atom types $S^4Zn^AZn^C{}_3$ (superscript *numerals* in the atom labels are co-ordination numbers). Atom Zn^A is co-ordinated also to three μ_3-S atoms, S^{3A}, each of which is connected to two further Zn atoms, Zn^B. The six Zn^B atoms constitute a slightly puckered

Table 1 Crystallographic data for $[Zn_{10}S_7(py)_9(SO_4)_3]\cdot 3H_2O$

M	1932.3
Crystal description	{100}{012}
Crystal symmetry	Monoclinic
Space group	$P2_1/c$
a/Å	11.279(6)
b/Å	23.419(6)
c/Å	27.26(1)
β/°	107.74(2)
U/Å^3	6858(5)
F(000)	3856
T/°C	21(1)
Z	4
D_c/g cm^{-3}	1.87
Radiation, λ/Å	Mo-Kα, 0.7107
μ/cm^{-1}	38.76
Crystal dimensions/mm	0.06 × 0.10 × 0.10
Scan mode	θ–2θ
$2\theta_{max}$/°	40
ω Scan angle/°	0.50 + 0.35 tan θ
No. intensity measurements	8854
Criterion for observed reflection	$I/\sigma(I) > 3$
No. independent observed reflections	4610
No. reflections (m) and variables (n) in final refinement	4610, 483
$R = \Sigma^m\|\Delta F\|/\Sigma^m\|F_o\|$	0.034
$R' = [\Sigma^m w\|\Delta F\|^2/\Sigma^m w\|F_o\|^2]^{\frac{1}{2}}$	0.039
$s = [\Sigma^m w\|\Delta F\|^2/(m-n)]^{\frac{1}{2}}$	1.10
Crystal decay	1 to 0.90
Maximum, minimum transmission coefficients	0.81, 0.65
R for 266 multiple measurements ($h0l$, $\bar{h}0l$)	0.019
Largest peak in final difference map/e Å^{-3}	0.65

hexagon. Thus the Zn_{10} array is effectively a Zn_4 tetrahedron $\{Zn^AZn^C{}_3\}$ crowned with a $Zn^B{}_6$ hexagon. Three of the edges of this $Zn^B{}_6$ hexagon are bridged by another set of three μ_3-S atoms, S^{3B}, back to the Zn^C atoms at the base of the tetrahedron. The six μ_3-S atoms in two sets all bridge the edges of the $Zn^B{}_6$ hexagon: S^{3A} atoms bridge in an upper plane [see Fig. 2(a)] to Zn^A, while S^{3B} atoms bridge downwards [see Fig. 2(a)] to Zn^C. This fulfils only two of the co-ordination positions at Zn^B and Zn^C: in order to complete the four-fold co-ordination of Zn, the three sulfate ions function as tripodal ligands, linking two Zn^B and one Zn^C, and there is one terminal pyridine ligand on each of Zn^B and Zn^C.

The composition of the cluster is $S^4Zn^AZn^C{}_3Zn^B{}_6S^{3A}{}_3S^{3B}{}_3(\mu_3\text{-}O_3SO)_3(py)_9$. Each of the Zn atom types has pseudo-tetrahedral co-ordination, specifically: $Zn^AS^4S^{3A}{}_3$; $Zn^BS^{3A}S^{3B}O^B(py^B)$; $Zn^CS^4S^{3B}O^C(py^C)$. Dimensions of the cluster according to these types of atoms are in Table 2, with mean values. The Zn–S^3 distances are in the range 2.27–2.35 Å, while the Zn–S^4 distances are *ca.* 0.15 Å longer, as is normal for increased co-ordination of the sulfide ligand. The Zn–N distances are close to 2.06 Å, and the mean of the Zn–O distances is 2.02 Å. Angles at the Zn atoms are within 2° of tetrahedral at Zn^A, but range up to 18° from tetrahedral for Zn^B and 12° from tetrahedral for Zn^C.

All of the non-terminal atoms in this structure would be expected to have ideal tetrahedral or part-tetrahedral local stereochemistry, and so in view of the observed deviations from tetrahedral angles we have questioned whether the core could approach more closely the tetrahedral ideal. To answer this we idealised the structure by computer-minimising the deviations of the angles at core atoms from 109.5°, while fixing the observed bond lengths. It is not possible to achieve tetrahedral angles throughout, for reasons of connectivity and different bond lengths, and the idealised structure is very similar to that observed. The core of $[Zn_{10}S_7(py)_9(SO_4)_3]$ is comprised of eight-membered rings (Zn^A–S^4–Zn^C–O^C–S^O–O^B–Zn^B–S^{3A}, S^4–Zn^C–O^C–S^O–O^B–Zn^B–S^{3B}–Zn^C) fused with six-membered rings (Zn^A–S^4–Zn^C–S^{3B}–Zn^B–S^{3A}, Zn^B–O^B–S^O–O^C–Zn^C–S^{3B}, Zn^B–O^B–S^O–O^B–Zn^B–S^{3B}), which is the source of the distortions from an idealised tetrahedral lattice. This connectivity of the core is discussed further below.

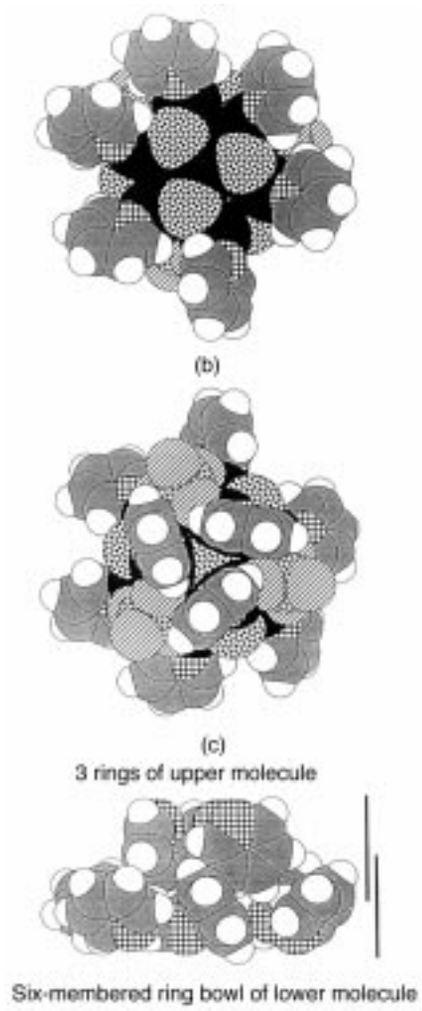

Fig. 3 Space-filling representations of the upper and lower axial surfaces of $[Zn_{10}S_7(py)_9(SO_4)_3]$, and the supramolecular interactions of the pyridine rings of cluster molecules stacked along the *a* axis. Atom shading as in Fig. 2: Zn, black; S, speckled; N, hatched; O, diagonally striped; C, grey; H, white. (a) The upper surface and the bowl formed by the six splayed pyridine rings of type B. (b) The lower surface of three pyridine rings of type C, parallel to the three-fold axis and engaged in mutual vertex-to-face attractive interactions. (c) Side view (*a* axis vertical) of the nine pyridine rings closely interacting at the interface of two molecules

Crystal supramolecularity

The crystal packing is determined by two significant features, one hydrophobic and the other hydrophilic. The hydrophobic interactions involve the pyridine rings, while the hydrophilic interactions involve the sulfate ions, hydrogen-bonded water molecules, and one type of sulfide ligand. As is apparent from Fig. 3(a), the six pyridine rings of type B are splayed like a bowl at the top of the cluster, while the three type C pyridine rings which are perpendicular to the lower surface of the cluster are aligned close to the three-fold axis [Fig. 3(b)]. These three type C pyridine rings have an intramolecular cycle of vertex-to-face attractive interactions, in which partially positive H atoms are directed towards partially negative C atoms. In the crystal the clusters are stacked (by translation along the *a* axis) such that the trio of pyridine rings of one cluster nestles in the bowl of its neighbour. Fig. 3(c) shows just these nine pyridine rings at the interface of two molecules. There are many specific intercluster

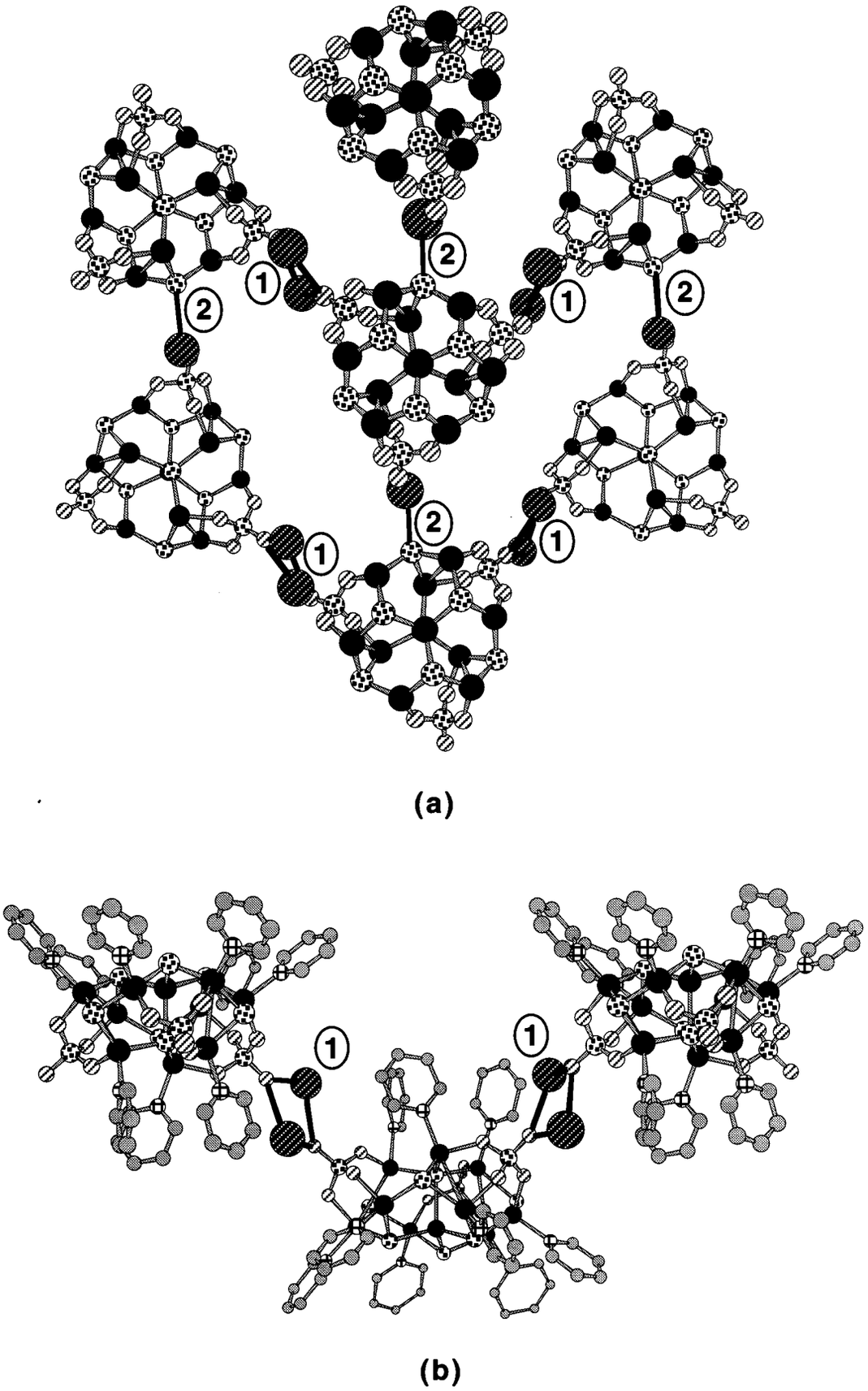

Fig. 4 Hydrogen bonding and lattice organisation in $[Zn_{10}S_7(py)_9(SO_4)_3]\cdot 3H_2O$. Water molecules are represented as diagonally striped enlarged spheres, hydrogen bonds as black lines, and the two types of hydrogen bonds are identified. (a) The pseudo-hexagonal net of hydrogen-bonded clusters around one cluster: pyridine rings are omitted for clarity. (b) View approximately perpendicular to that in (a), showing how type 1 hydrogen bonds link molecules alternating up and down in corrugated layers

edge-to-face attractive interactions in this hydrophobic region, which has some similarity with inclusions in calixarenes and other aromatic hosts.[49]

The equatorial belt of $[Zn_{10}S_7(py)_9(SO_4)_3]$ which is not covered by pyridine rings has protruding O_3SO^{2-} groups, and these are linked by hydrogen-bonding water molecules. There

Table 2 Selected distances (Å) and angles (°)

	Range	Mean
Zn^{A}–S^{4}	2.453(2)	2.453
Zn^{C}–S^{4}	2.314(3), 2.321(3), 2.329(3)	2.321
Zn^{A}–S^{3A}	2.330(3), 2.334(3), 2.353(3)	2.339
Zn^{B}–S^{3A}	2.267(3), 2.273(3), 2.273(3), 2.278(3), 2.284(3), 2.290(3)	2.278
Zn^{B}–S^{3B}	2.277(3), 2.280(3), 2.284(3), 2.288(3), 2.290(3), 2.292(3)	2.285
Zn^{B}–N^{B}	2.059(3), 2.060(3), 2.060(3), 2.061(3), 2.061(3), 2.061(3)	2.060
Zn^{C}–N^{C}	2.059(3), 2.059(3), 2.060(3)	2.059
Zn^{C}–O^{C}	1.997(6), 2.008(6), 2.015(6)	2.006
Zn^{B}–O^{B}	1.995(6), 2.020(6), 2.023(6), 2.044(6), 2.057(6), 2.061(6)	2.033
S^{4}–Zn^{A}–S^{3A}	107.2(1), 107.3(1), 108.5(1)	107.7
S^{3A}–Zn^{A}–S^{3A}	110.8(1), 111.0(1), 111.8(1)	111.2
S^{3A}–Zn^{B}–S^{3B}	122.2(1), 123.3(1), 124.0(1), 125.0(1), 125.5(1), 127.8(1)	124.6
S^{4}–Zn^{C}–S^{3B}	119.3(1), 120.1(1), 121.1(1)	120.2
Zn^{A}–S^{4}–Zn^{C}	103.2(1), 103.2(1), 103.5(1)	103.3
Zn^{C}–S^{3B}–Zn^{B}	87.4(1), 88.1(1), 88.3(1), 89.1(1), 99.4(1), 99.5(1)	92.0
Zn^{C}–S^{4}–Zn^{C}	114.2(1), 114.6(1), 115.8(1)	114.9
Zn^{B}–S^{3A}–Zn^{B}	100.8(1), 102.1(1), 102.9(1)	101.9
Zn^{A}–S^{3A}–Zn^{B}	99.9(1), 101.9(1), 102.3(1), 104.5(1), 105.0(1), 105.3(1)	103.2
Zn^{B}–S^{3B}–Zn^{B}	105.3(1), 105.9(1), 109.1(1)	106.8
S^{4}–Zn^{C}–O^{C}	105.2(2), 106.7(2), 107.3(2)	106.4
S^{4}–Zn^{C}–N^{C}	107.1(2), 109.2(2), 110.3(2)	108.9
S^{3B}–Zn^{C}–O^{C}	108.1(2), 108.3(2), 111.4(2)	109.3
S^{3B}–Zn^{C}–N^{C}	112.3(2), 113.7(2), 115.5(2)	113.8
O^{C}–Zn^{C}–N^{C}	93.6(3), 95.0(2), 96.9(2)	95.2
O^{B}–Zn^{B}–N^{B}	88.6(2), 91.9(2), 95.8(3), 96.0(3), 98.7(2), 102.5(2)	95.6
S^{3B}–Zn^{B}–O^{B}	100.2(2), 101.1(2), 101.2(2), 102.7(2), 102.9(2), 105.8(2)	102.3
S^{3A}–Zn^{B}–O^{B}	108.5(2), 109.1(2), 109.8(2), 113.0(2), 114.2(2), 115.3(2)	111.7
S^{3B}–Zn^{B}–N^{B}	105.5(2), 109.9(2), 112.4(2), 113.7(2), 115.8(2), 117.7(2)	112.5
S^{3A}–Zn^{B}–N^{B}	100.8(2), 103.5(2), 105.0(2), 107.9(2), 108.1(2), 110.7(2)	106.0

are two hydrogen-bonding motifs: in motif **1** a pair of water molecules forms an O_4 cycle with two sulfate O atoms (O · · · O distances 2.81, 2.84, 2.93, 2.95 Å). In the other motif, **2**, a water molecule is hydrogen-bonded to a sulfate O and to a S^{3B} atom (O · · · O 2.73, O · · · S 3.29 Å).

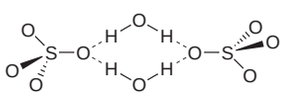

1

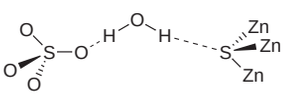

2

Fig. 4 provides further information about the crystal packing, showing that the hydrogen bonding connects the clusters in a puckered pseudo-hexagonal net, which is a consequence of the fact that the terminal S–O bonds are inclined at about 45° to the pseudo-three-fold axis (crystallographic *a* axis) and therefore the hydrogen-bonding connections are also similarly directed. The pseudo-hexagonal net results because each cluster is hydrogen bonded to six others, three by type **1** hydrogen bonds and three by type **2** hydrogen bonds. These two types of hydrogen bonds are included in opposite senses relative to the cluster three-fold axis.

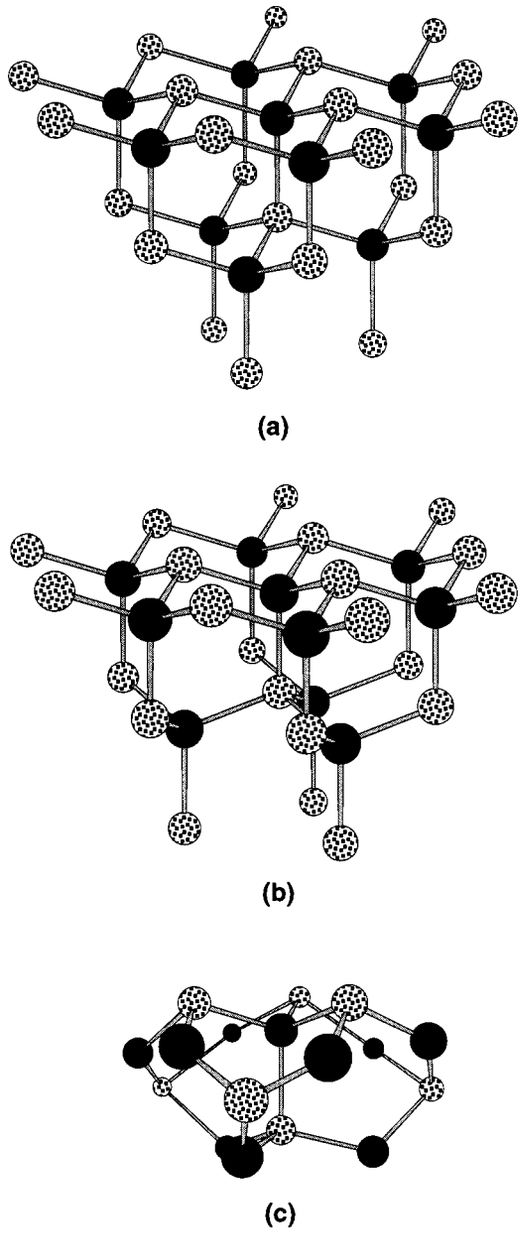

Fig. 5 Comparative views of appropriate fragments of the (a) cubic (sphalerite) and (b) hexagonal (wurtzite) lattices of ZnS and (c) the core of $[Zn_{10}S_7(py)_9(SO_4)_3]$

Relationship to metal chalcogenide lattice fragments and clusters

The Zn–S connectivity in $[Zn_{10}S_7(py)_9(SO_4)_3]$ is not that of any of the established metal–sulfide lattices. Fig. 5 shows appropriate fragments of the cubic (sphalerite) and hexagonal (wurtzite) lattices of ZnS, in comparison with the core of $[Zn_{10}S_7(py)_9(SO_4)_3]$. In each fragment there is a centred hexagon of Zn atoms in one layer and a triangle of Zn in the underneath layer, arranged around a S^4–Zn bond connecting the layers. The difference between the sphalerite and wurtzite structures can be described in terms of the staggered or eclipsed conformation (respectively) about this S^4–Zn bond: in the core of $[Zn_{10}S_7(py)_9(SO_4)_3]$ the conformation is neither of these, but is closer to staggered. The feature of $[Zn_{10}S_7(py)_9(SO_4)_3]$ not present in either of the other lattices is the occurrence of S atoms (S^{3B}) which bridge Zn atoms in adjacent layers in a manner which converts the Zn_3S_3 chairs of both sphalerite and wurtzite into Zn_3S_3 rings in envelope conformation. This is best illustrated by demonstrating the changes which convert the $Zn_{10}S_{22}$ fragment of sphalerite into the cluster $[Zn_{10}S_7(py)_9]$, as shown in Fig. 6.

There are nine S^2 atoms in $Zn_{10}S_{22}$, and they are floppy connectors. Six of these [S^{2e} in Fig. 6(a)] are removed, and the other

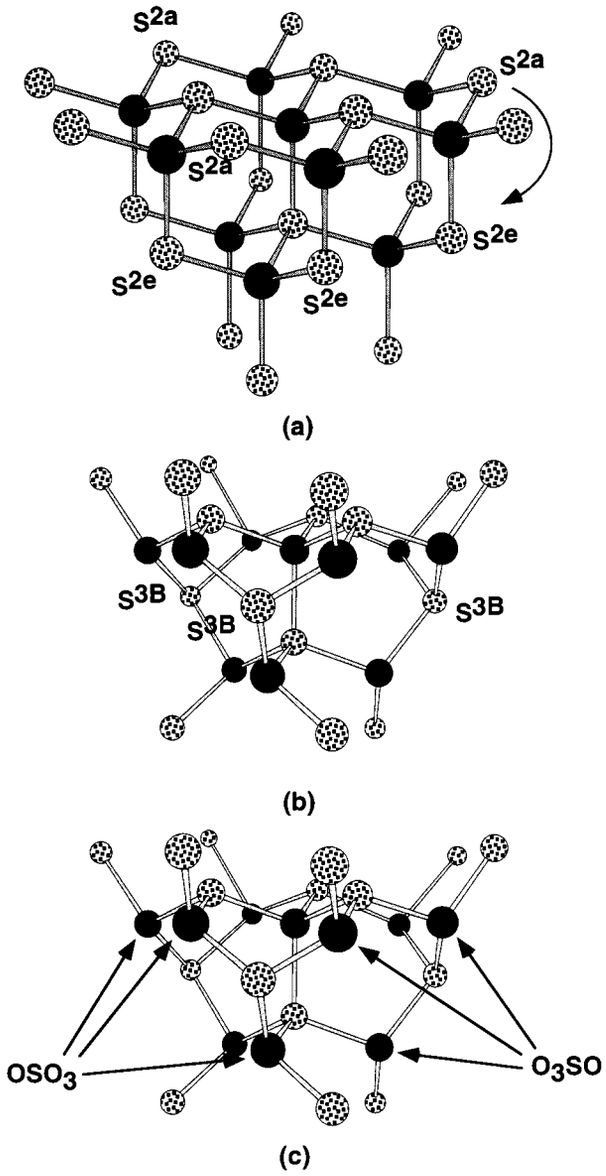

Fig. 6 Construction of $[Zn_{10}S_7(py)_9(SO_4)_3]$ from the $Zn_{10}S_{22}$ core of sphalerite (see text description). Part (a) identifies three of the S^{2e} atoms (six in total) which are removed, and the S^{2a} atoms (three) which are folded down (arrow) to become S^{3B} [in part (b)]. Part (c) shows how two of the three SO_4^{2-} ions cap Zn_3 faces. The terminal S atoms in (a) become the pyridine N atoms of $[Zn_{10}S_7(py)_9(SO_4)_3]$

three (S^{2a}) are folded down to become the S^{3B} atoms connecting Zn^B and Zn^C [see Fig. 6(b)]. The composition is then $Zn_{10}S_{16}$. There are nine terminal S atoms which will become the N atoms of the pyridine ligands. Even though the nine Zn^B and Zn^C atoms in Fig. 6(b) are only three-connected, this structure was geometrically idealised to the requirement of tetrahedral or part-tetrahedral co-ordination at all non-terminal atoms, yielding the geometry shown in Fig. 6(c). This is in fact remarkably similar to that of the $Zn_{10}S_7(py)_9$ core of $[Zn_{10}S_7(py)_9(SO_4)_3]$, with the zinc–pyridine bonds appropriately arrayed. With a small torsion about the three-fold axis the three tripodal O_3SO^{2-} ions can complete the tetrahedral co-ordination of all Zn^B and Zn^C atoms [see Fig. 6(c)].

A different structural feature for Group 12 metal chalcogenide clusters occurs in the sulfide–thiolate cluster $[Cd_{17}S_4(SR)_{28}]^{2-}$ [22,50,51] and derivatives,[52,53] and in $[Cd_{32}E_{14}(ER)_{36}L_4]$ (E = S or Se, L = dmf[43] or PPh_3[54]), which is the next higher structural homologue of $[Cd_{17}S_4(SR)_{28}]$.[55] While the cores of these tetrahedral clusters are fragments of sphalerite, the vertices contain the barrelenoid moiety which is characteristic of the

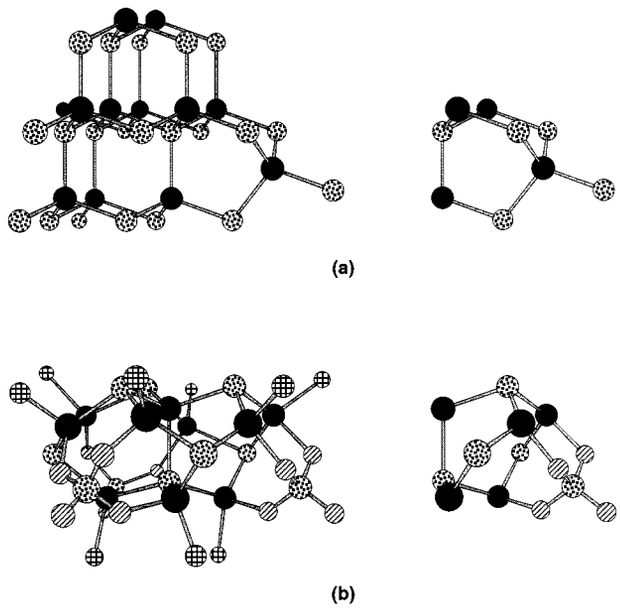

Fig. 7 Comparative views of the contrasting connectivities of the tripodal vertices of (a) the Cd_{17} and Cd_{32} clusters and (b) $[Zn_{10}S_7(py)_9(SO_4)_3]$. (a) Part of the cluster geometry present in Cd_{17} and Cd_{32}, with the barrelenoid vertex exploded. (b) The connectivity of $[Zn_{10}S_7(py)_9(SO_4)_3]$ with the O_3SO vertex exploded. Note the reversed polarities of the vertical M–S bonds

wurtzite lattice rather than the sphalerite lattice (which is comprised of fused adamantanoid cages only). This barrelenoid feature at a cluster vertex is illustrated in Fig. 7(a), which shows the $(\mu\text{-}S)_3ML$ tripodal cap to an M_3 ring. In $[Zn_{10}S_7(py)_9(SO_4)_3]$ the O_3SO tripodal ligand on a Zn_3 ring is connected quite differently to the core of the cluster, and there is no analogous barrelenoid cage, as shown in Fig. 7(b).

Yet another ZnS cluster framework occurs in $[Zn_{10}Et_{10}(SEt)_{10}]$.[25] Each Zn atom has tetrahedral co-ordination, with a terminal Et ligand, and each SEt thiolate ligand is triply bridging, but the Zn–S connectivity of the core is not related to those discussed in this paper.

Acknowledgements

We are grateful for the funding of this research by the Australian Research Council.

References

1 I. G. Dance and K. J. Fisher, *Prog. Inorg. Chem.*, 1994, **41**, 637.
2 I. G. Dance, A. Choy and M. L. Scudder, *J. Am. Chem. Soc.*, 1984, **106**, 6285.
3 A. Choy, D. C. Craig, I. G. Dance and M. L. Scudder, *J. Chem. Soc., Chem. Commun.*, 1982, 1246.
4 I. G. Dance, *Aust. J. Chem.*, 1985, **38**, 1745.
5 G. S. H. Lee, Ph.D. Thesis, University of New South Wales, 1992.
6 B. Krebs and G. Henkel, *Angew. Chem., Int. Ed. Engl.*, 1991, **30**, 769.
7 M. D. Nyman, M. J. Hampden-Smith and E. N. Duesler, *Inorg. Chem.*, 1996, **35**, 802.
8 D. Johnstone, J. E. Fergusson and W. T. Robinson, *Bull. Chem. Soc. Jpn.*, 1972, **45**, 3721.
9 K. S. Hagen, D. W. Stephan and R. H. Holm, *Inorg. Chem.*, 1982, **21**, 3928.
10 J. L. Hencher, M. Khan, F. F. Said and D. G. Tuck, *Inorg. Nucl. Chem. Lett.*, 1981, **17**, 287.
11 J. J. Vittal, *Polyhedron*, 1996, **15**, 1585.
12 P. A. W. Dean and J. J. Vittal, *Inorg. Chem.*, 1987, **26**, 278.
13 P. A. W. Dean, J. J. Vittal and N. C. Payne, *Inorg. Chem.*, 1987, **26**, 1683.
14 I. G. Dance, *Polyhedron*, 1986, **5**, 1037.
15 I. G. Dance, *J. Chem. Soc., Chem. Commun.*, 1980, 818.
16 I. G. Dance, *J. Am. Chem. Soc.*, 1980, **102**, 3445.

17 A. H. Robbins, D. E. McRee, M. Williamson, S. A. Collett, N. H. Xuong, W. F. Furey, B. C. Wang and C. D. Stout, *J. Mol. Biol.*, 1991, **221**, 1269.
18 J. D. Otvos, C. F. Shaw and D. H. Petering, *Comments Inorg. Chem.*, 1989, **9**, 1.
19 M. J. Stillman and A. J. Zelazowski, *Biochem. J.*, 1989, **262**, 181.
20 T. Lover, W. Henderson, G. A. Bowmaker, J. M. Seakins and R. P. Cooney, *Inorg. Chem.*, 1997, **36**, 3711.
21 T. Lover, G. A. Bowmaker, W. Henderson and R. P. Cooney, *Chem. Commun.*, 1996, 683.
22 T. Lover, W. Henderson, G. A. Bowmaker, J. M. Seakins and R. P. Cooney, *Chem. Mater.*, 1997, **9**, 1878.
23 G. W. Adamson and H. M. M. Shearer, *Chem. Commun.*, 1969, 897.
24 G. W. Adamson, N. A. Bell and H. M. M. Shearer, *Acta Crystallogr.*, *Sect. B*, 1982, **38**, 462.
25 D. Zeng, M. J. Hampden-Smith and E. N. Duesler, *Inorg. Chem.*, 1994, **33**, 5376.
26 L. E. Brus, *J. Phys. Chem.*, 1986, **90**, 2555.
27 A. Henglein, *Chem. Rev.*, 1989, **89**, 1861.
28 Y. Wang and N. Herron, *J. Phys. Chem.*, 1991, **95**, 525.
29 M. L. Steigerwald and L. E. Brus, *Annu. Rev. Mater. Sci.*, 1989, **19**, 471.
30 A. Henglein, *Top. Curr. Chem.*, 1988, **143**, 113.
31 M. L. Steigerwald and L. E. Brus, *Acc. Chem. Res.*, 1990, **23**, 183.
32 D. M. Wilhelmy and E. Matijevic, *J. Chem. Soc.*, *Faraday Trans. 1*, 1984, 563.
33 K. Osakada, A. Taniguchi, E. Kubota, S. Dev, K. Tanaka, K. Kubota and T. Yamamoto, *Chem. Mater.*, 1992, **4**, 562.
34 H. C. Youn, S. Baral and J. H. Fendler, *J. Phys. Chem.*, 1988, **92**, 6320.
35 A. R. Kortan, R. Hull, R. L. Opila, M. G. Barwendi, M. L. Steigerwald, P. J. Carroll and L. E. Brus, *J. Am. Chem. Soc.*, 1990, **112**, 1327.
36 X. K. Zhao, S. Baral, R. Rolandi and J. H. Fendler, *J. Am. Chem. Soc.*, 1988, **110**, 1012.
37 S. Baral and J. H. Fendler, *J. Am. Chem. Soc.*, 1989, **111**, 1604.
38 V. Sankaran, J. Yue, R. E. Cohen, R. R. Schrock and R. J. Silbey, *Chem. Mater.*, 1993, **5**, 1133.
39 J. Bucheler, N. Zeug and H. Kisch, *Angew. Chem.*, *Int. Ed. Engl.*, 1982, **21**, 783.
40 J. Muilu and T. A. Pakkanen, *Appl. Surf. Sci.*, 1994, **75**, 75.
41 J. Muilu and T. A. Pakkanen, *Surf. Sci.*, 1996, **364**, 439.
42 W. E. Farneth, N. Herron and Y. Wang, *Chem. Mater.*, 1992, **4**, 916.
43 N. Herron, J. C. Calabrese, W. E. Farneth and Y. Wang, *Science*, 1993, **259**, 1426.
44 J. de Meulenaer and H. Tompa, *Acta Crystallogr.*, 1965, **19**, 1014.
45 A. D. Rae, RAELS, A Comprehensive Constrained Least Squares Refinement Program, University of New South Wales, 1989.
46 A. K. Verma, T. B. Rauchfuss and S. R. Wilson, *Inorg. Chem.*, 1995, **34**, 3072.
47 A. Müller, U. Schimanski and H. Bögge, *Z. Naturforsch.*, *Teil B*, 1985, **40**, 1277.
48 H. Li, S. Du and X. Wu, *Acta Crystallogr.*, *Sect. C*, 1994, **50**, 498.
49 J. L. Atwood, G. A. Koutsantonis and C. L. Raston, *Nature* (*London*), 1994, **368**, 229.
50 G. S. H. Lee, D. C. Craig, I. N. L. Ma, M. L. Scudder, T. D. Bailey and I. G. Dance, *J. Am. Chem. Soc.*, 1988, **110**, 4863.
51 T. Lover, G. A. Bowmaker, J. M. Seakins and R. P. Cooney, *Chem. Mater.*, 1997, **9**, 967.
52 X. Jin, K. Tang, S. Jia and Y. Tang, *Polyhedron*, 1996, **15**, 2617.
53 T. Vossmeyer, G. Reck, L. Katsikas, E. T. K. Haupt, B. Schulz and H. Weller, *Science*, 1995, **267**, 1476.
54 S. Behrens, M. Bettenhausen, A. C. Deveson, A. Eichhofer and D. Fenske, *Angew. Chem.*, *Int. Ed. Engl.*, 1996, **35**, 2215.
55 I. G. Dance, in preparation.

Received 3*rd November* 1997; *Paper* 7/07873K